Optical Tweezers

Experiment OT - sjh,rd

University of Florida — Department of Physics
PHY4803L — Advanced Physics Laboratory

Objective

An optical tweezers apparatus uses a tightly focused laser to generate a trapping force that can capture and move small particles under a microscope. Because it can precisely and non-destructively manipulate objects such as individual cells and their internal components, the optical tweezers is extremely useful in biological physics research. In this experiment you will use optical tweezers to trap small silica spheres immersed in water. You will learn how to measure and analyze the frequency spectrum of their Brownian motion and their response to hydrodynamic drag in order to characterize the physical parameters of the optical trap with high precision. The apparatus can then be used to measure a microscopic biological force, such as the force that propels a swimming bacterium or the force generated by a transport motor operating inside a plant cell.

References

D.C. Appleyard *et al.*, *Optical trapping for undergraduates*, Am. J. Phys. **75** 5-14 (2007).

A. Ashkin, *Acceleration and Trapping of Particles by Radiation Pressure*, Phys. Rev. Lett. **24** 156-159 (1970).

K. Berg-Sorensen and H.Flyvbjerg, *Power spectrum analysis for optical tweezers*, Rev. Sci. Instr. **75** 594-612 (2004).

S. Chattopadhyay, R. Moldovan, C. Yeung, X.L. Wu, *Swimming efficiency of bacterium Escherichia coli*, Proc. Nat. Acad. Sci. USA **103** 13712-13717 (2006).

Daniel T. Gillespie *The mathematics of Brownian motion and Johnson noise*, Amer. J. of Phys. **64** 225 (1996).

Daniel T. Gillespie *Fluctuation and dissipation in Brownian motion*, Amer. J. of Phys. **61** 1077 (1993).

S.F. Tolic-Norrelykke, et al., *Calibration of optical tweezers with positional detection in the back focal plane*, Rev. Sci. Instr. **77** 103101 (2006).

University of California, Berkeley advanced lab wiki site on optical trapping: www.advancedlab.org/mediawiki/index.php/Optical_Trapping is one of the best references for this experiment. Be sure to check it out!

Introduction

The key idea of optical trapping is that a laser beam brought to a sharp focus generates a restoring force that can pull particles into that

focus. Arthur Ashkin demonstrated the principle in 1970 and reported on a working apparatus in 1986. The term optical trapping often refers to laser-based methods for holding neutral atoms in high vacuum, while the term optical tweezers (or laser tweezers) typically refers to the application studied in this experiment: A microscope is used to bring a laser beam to a sharp focus inside an aqueous sample so that microscopic, non-absorbing particles such as small beads or individual cells can become trapped at the beam focus. Optical tweezers have had a dramatic impact on the field of biological physics, as they allow experimenters to measure non-destructively and with high precision the tiny forces generated by individual cells and biomolecules. This includes propulsive forces generated by swimming bacteria, elastic forces generated by deformation of biomolecules, and the forces generated by processive enzyme motors operating within a cell. Experimenting with an apparatus capable of capturing, transporting, and manipulating individual cells and organelles provides an intriguing introduction to the world of biological physics.

A photon of wavelength λ and frequency $f = c/\lambda$ carries an energy $E = hf$ and a momentum of magnitude $p = h/\lambda$ in the direction of propagation (where h is Planck's constant and c is the speed of light). Note that our laser power—up to 30 mW—focused down to a few square microns, implies laser intensities over 10^6 W/cm^2 at the beam focus. Particles that absorb more than a tiny fraction of the incident beam will absorb a large amount of energy relative to their volume rather quickly. In fact, light-absorbing particles can be quite rapidly vaporized (opticuted) by the trapping laser. (Incidentally, your retina contains many such particles - see *Laser Safety* below). While the scatterer and surrounding fluid always absorbs some energy, our infrared laser wavelength ($\lambda = 975$ nm) is specifically chosen because it is where absorption in water and most biological samples is lowest. The absorption rate is also near a minimum for the silica spheres you will study. You should keep an eye out for evidence of heating in your samples, but because of the relatively low absorption rate and because the particles have good thermal conductance with the surrounding water, effects of heating should be modest.

The theory and practice of laser tweezers are highly developed and numerous excellent reviews, tutorials, simulations, and other resources on the subject are easy to find online.

Physics of the trapped particle

The design, operation, and calibration of our laser tweezers draws on principles of optics, mechanics and statistical physics. We begin with an overview of the physics relevant to generating the trapping force and for calibrating the restoring and viscous damping forces associated with its operation.

The laser force arises almost entirely from the elastic scattering of laser photons whereby the particle alters the direction of the photon momentum without absorbing any of its energy. It is typically decomposed into two components: (1) a gradient force that everywhere points toward higher laser intensities and (2) a weaker scattering force in the direction of the photon flow. For the sharply focused laser field of an optical tweezers, the gradient force points toward the focus and provides the Hooke's law restoring force responsible for trapping the particle. The scattering force is in the direction of the laser beam and simply shifts the trap equilibrium position slightly downstream of the laser focus.

The origin of both forces is similar: the particle elastically scatters a photon and alters its

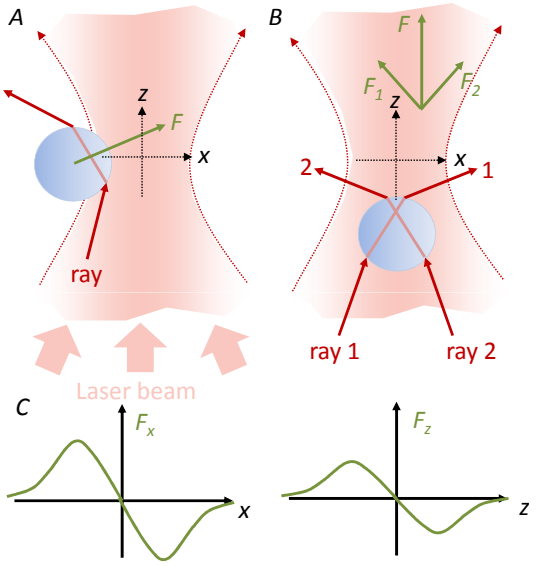

Figure 1: Ray model for the trapping force at the focus of a laser beam. A particle displaced horizontally *(A)* or vertically *(B)* from the focus (at $x = y = z = 0$) refracts the light away from the focus, leading to a reaction force that pulls the particle toward the focus; *(C)* Schematic of the restoring forces F_x and F_z versus displacement x and z of the particle from the trap center. Near the beam focus, $F_x \approx -kx$ and $F_z \approx -k'z$.

momentum. Momentum conservation implies that the scattered photon imparts an equal and opposite momentum change to the particle. The net force on the particle is a vector equal and opposite the net rate of change of momentum of all the scattered laser photons.

For particles with diameters d large compared to λ, the ray optics of reflection and refraction at the surface of the sphere provide a good model for the laser forces. The ray drawings in Figure 1 illustrate how laser beam refraction generates a trapping force. The laser beam is directed in the positive z-direction and brought to a focus by a microscope objective. Note that, owing to wave diffraction, the focal region has nonzero width in the xy direction. Near the beam focus, a spherical dielectric particle alters the direction of a ray by refracting it as shown in 1A. Momentum conservation implies that the particle experiences a force, indicated by $\mathbf{F}$ in the figure, that is directed toward the beam focus. If the particle is located below the focus, it refracts the converging rays (such as rays 1 and 2) as shown in 1B. The corresponding reaction forces $\mathbf{F}_1$ and $\mathbf{F}_2$ acting on the particle give a vector sum $\mathbf{F}$ that is again directed toward the laser focus. The net result of all the refractive scattering at any location in the vicinity of the focus results in the gradient force that pulls the particle into the beam focus. Reflection at the boundaries between the sphere and the medium results in the scattering force in the direction of the laser photons.

For smaller particles of diameter $d \ll \lambda$, Rayleigh scattering describes the interaction: The particle acts as a point dipole, scattering the incident beam in a spatially dependent fashion that depends on the particle's location in the laser field. The result is a net force $\mathbf{F}$ given by

$$\mathbf{F} = \alpha \left(\frac{1}{2} \nabla E^2 + \frac{d}{dt} (\mathbf{E} \times \mathbf{B}) \right) \qquad (1)$$

where $\mathbf{p} = \alpha \mathbf{E}$ gives the particle's induced dipole moment. The first term is in the direction of the gradient of the field intensity, i.e., the trapping force directed toward the laser focus. The second term gives the weaker scattering force—in the direction of the field's Poynting vector $\mathbf{E} \times \mathbf{B}$.

The center of the trap will be taken as $\mathbf{r} = 0$. For any small displacement (any direction) away from the trap center, the particle is subject to a Hooke's law restoring force, i.e., proportional to and opposite the displacement. Detailed calculations show that the force constant is sensitive to the shape and intensity of the laser field, the size and shape

of the trapped particle, and the optical properties of the particle and surrounding fluid. Consequently, the Hooke's law force is difficult to predict. Furthermore, our apparatus operates in an intermediate regime of particle sizes where neither the ray optics nor Rayleigh models are truly appropriate. The diameter d of the silica spheres (SiO_2) range in size from 0.5-5 μm. Thus with the laser wavelength of $\lambda = 975$ nm, we have $d \sim \lambda$. Fortunately, we do not need to calculate or predict the Hooke's law force constants based on these scattering models. Instead, you will learn how to determine them in situ—from measurements made with the particle in the trap.

Consider the motion and forces in terms of their components. The laser beam in our apparatus is directed vertically upward, which will be taken as the $+z$ direction so that the x and y coordinates then describe the horizontal plane. Because the laser beam and focusing optics are cylindrically symmetric around the z-axis, the trap has the same properties in the x-direction as in the y-direction. We need only consider the equations for the x motion of the particle, and a similar set of equations will describe the motion in the y-direction. However, the trapping force that acts along the z direction is different than for x and y, as the laser intensity in the focal region is clearly not a spherically symmetric pattern. The width of the beam focus in its radial (xy) dimension is very narrow. It is limited by wave diffraction to roughly one wavelength ($\lambda \sim 1\mu$m), whereas this is not the case in z. Hence the restoring force in z is not necessarily as strong as in xy.

If the focal "cone" has too shallow an angle (technically, a large f-number or small *numerical aperture*), particles may be trapped in the xy direction but not trapped along z. The laser beam will tend to pull small particles in toward the central optical axis and then push them up and out of the trap. By employing a large numerical aperture, our apparatus provides excellent trapping in all three directions.

We will investigate the motions of the particle in the xy directions only. Consequently, in the discussion that follows, when forces, impulses, velocities or other vector quantities are written without vector notation (e.g., F instead of $\mathbf{F}$) and without explicit directional subscripts (e.g., $F_z = -k'z$), they represent the x-component of the corresponding vector quantity. For example, the trapping force in the x-direction is simply $F_{\text{trap}} = -kx$.

What other forces act on the particle? The laser in our apparatus is directed vertically upward—along the same axis as gravitational and buoyant forces. Both silica spheres and bacteria are more dense than water and thus experience a net downward force from these sources. A constant force in the z-direction shifts the equilibrium position along the z-axis but leaves the force constant unmodified. For example, the gravitational force on a mass m hanging from a mechanical spring of force constant k shifts the equilibrium by an amount $-mg/k$, but the net force $F = -kz$ still holds with z now the displacement from the new equilibrium point. Thus, the $F_x = -kx$, $F_y = -ky$, $F_z = -k'z$ "trapping force" can and will be taken as relative to the final equilibrium position and includes not only the true trapping force centered at the laser focus, but also the laser scattering force and the forces due to gravity and buoyancy. Keep in mind that these other forces are relatively weak compared to the true trapping force and so the shift in the equilibrium position from the laser focus is rather small.

The fluid environment supplies two additional and significant forces to the particle. The particles that we study with our laser tweezers are suspended in water where molecules are in constant thermal motion, i.e.,

they are moving with a range of speeds in random directions. For still water with no bulk flow, the x-component of velocity (or the component along any axis) is equally likely to be positive as negative and will have an expectation value of zero: $\langle v_x \rangle = 0$. Its mean squared value is nonzero, however, as the average kinetic energy of the gas is determined by the temperature T. More precisely the equipartition theorem states that the mean squared value of any component of the velocity, e.g. $\langle v_x^2 \rangle$, is related to the temperature T by

$$\frac{1}{2} m \langle v_x^2 \rangle = \frac{1}{2} k_B T \tag{2}$$

where temperature is measured in Kelvin and $k_B = 1.38 \times 10^{-23}$ J/K is Boltzmann's constant. The value of v_x for any given particle is a random variable whose probability distribution is known as the Maxwell-Boltzmann distribution:

$$P(v_x) dv_x = \frac{1}{\sqrt{2\pi\sigma_v^2}} \exp\left(-\frac{v_x^2}{2\sigma_v^2}\right) dv_x \tag{3}$$

$P(v_x)dv_x$ gives the probability that the velocity component v_x for a given particle lies in the range between v_x and $v_x + dv_x$. The Maxwell Boltzmann distribution is a Gaussian distribution whose variance $\sigma_v^2 = \langle v_x^2 \rangle = k_B T/m$ makes it satisfy the equipartition theorem. Likewise the other velocity components v_y and v_z obey the same distribution, (3), with the same variance σ_v^2.

Exercise 1 *(a) Find the root-mean-square (rms) velocity in three dimension* $\sqrt{\langle |\mathbf{v}|^2 \rangle} = \sqrt{\langle v_x^2 + v_y^2 + v_z^2 \rangle} = \sqrt{3k_B T/m}$ *for water molecules near room temperature (23 C). (b) Find the rms x-component of velocity,* $\sqrt{\langle v^2 \rangle} = \sigma_v$ *and the number density of water molecules (per unit volume). Use them to estimate the rate at which molecules cross through (in either direction) a 1 μm diameter disk oriented with its normal along the x-direction.*

Therefore, even if there is no bulk movement of the water, a small particle immersed in water is continuously subject to collisions from moving water molecules. The collisional force $\mathbf{F}_i(t)$ exerted on the particle during the ith collision delivers an impulse $\mathbf{J}_i = \int \mathbf{F}_i(t) dt$ to the particle over the duration of the collision. By the impulse-momentum theorem, this impulse changes the particle momentum by the same amount $\Delta\mathbf{p}_i = \mathbf{J}_i$; impulse is momentum change and they can be used somewhat interchangeably. For a one-micron particle in water at room temperature, such collisions occur at a rate $\sim 10^{19}$ per second. Over some short time interval Δt, the total impulse $\Delta\mathbf{p}$ delivered to the particle is the sum of the individual impulses: $\Delta\mathbf{p} = \sum_i \mathbf{J}_i$, and the average collisional force exerted on the particle over this interval is then $\mathbf{F}_c(t) = \Delta\mathbf{p}/\Delta t$.

Theory cannot predict the individual impulses. A head-on collision with a high velocity water molecule delivers a large impulse, while a glancing collision with a low velocity molecule delivers a smaller impulse. Depending on the direction of the collision, $\mathbf{J}_i$ can point in any direction. Even when summed over an interval Δt, $\Delta\mathbf{p}$ will include a random component.

When no other forces act on the particle, the impulses push the particle slowly through the fluid along a random, irregular trajectory. This random motion is known as *Brownian motion* and is readily observed under a microscope when any small (micron-sized or smaller) particle is suspended in a fluid. When the particle is trapped in an optical tweezers, the impulses act as a continuous perturbation that pushes the particle in random directions. Because of the random component of the force, the particle motion is said to be *stochastic* (governed by probability distributions), and

only probabilities or average behavior can be predicted.

Exercise 2 *You can estimate the average speed of Brownian motion from the fact that the speed of the microscopic particle at temperature T must also satisfy the equipartition theorem (2). For a silica sphere of diameter 1 μm and a density of 2.65 g/cm^3, what is its rms velocity at room temperature? Is your result still valid if the particle is in an optical trap?*

Note that if a particle moves through the fluid at a velocity $\mathbf{v}$, collisions are not equally likely in all directions. More collisions will occur on the side of the particle heading into the fluid than on the trailing side and the total impulse $\Delta\mathbf{p}$ that is acquired by the particle will acquire a non-zero mean. The direction of this impulse must tend to oppose the motion of the particle through the fluid. Macroscopically, we describe this effect by saying that the particle experiences a viscous drag force $\mathbf{F}_{\text{drag}}$ that is proportional to (and in opposite direction from) its velocity

$$\mathbf{F}_{\text{drag}} = -\gamma\mathbf{v} \tag{4}$$

where γ is the drag coefficient. As they have the same microscopic origin, there must be a connection between the magnitude of the small impulses $\Delta\mathbf{p}$ and the strength of the macroscopic drag force. We can find this connection by noting that while the microscopic collisions deliver momentum to the particle and drive its Brownian motion, the overall drag force tends to slow the particle down. On average these two effects must balance each other exactly, so that the particle neither slows to a halt nor accelerates indefinitely. Rather the particle maintains an average kinetic energy in accord with the equipartition theorem (Eq. 2). In the following we investigate this force balance in order to relate the magnitude of the microscopic impulses to the drag coefficient γ.

Therefore suppose that a micron-sized particle is moving through a fluid. For clarity we consider only one component (say x) of its motion, although exactly the same arguments wil apply to its motion in y and z. Let Δp represent the x-component of the net vector impulse $\Delta\mathbf{p}$ that is delivered to the particle during an interval Δt. Likewise v and p represent the x-component of the velocity and momentum, and J_i is the x-component of impulse from a single collision. Because of the high collision rate, Δt can be assumed short enough that the particle velocity over this interval is effectively constant, but still long enough to allow, say, a few thousand collisions or more—enough to apply the central limit theorem, which says that the sum $\Delta p = \sum_i \Delta p_i$ will be a random variable with a Gaussian probability distribution no matter what probability distribution governs J_i. Moreover, the Gaussian distribution will have a mean $\mu_p = \langle \Delta p \rangle$ equal to the number of collisions times the mean of the contributing J_i and it will have a variance $\sigma_p^2 = \langle (\Delta p - \mu_p)^2 \rangle$ equal to the number of collisions times the variance of the J_i. Because the number of collisions is proportional to Δt, both the mean μ_p and the variance σ_p^2 should be proportional to Δt.

The total impulse Δp is therefore a random variable that can be expressed as

$$\Delta p = \mu_p + \delta p \tag{5}$$

where μ_p is a constant (associated with the mean of the impulse distribution) and δp is a zero-mean Gaussian random variable: $\langle \delta p \rangle = 0$ with a non-zero variance $\langle \delta p^2 \rangle$ (associated with the variance of the impulse distribution).

In a still fluid with no bulk flow, a particle at rest ($v = 0$) experiences collisions from all directions equally. A collision delivering an

impulse Δp_i, is exactly as likely as a collision delivering $-\Delta p_i$. Consequently, Δp is equally likely to be positive as negative and its expectation value is zero: $\mu_p = 0$. However if the particle is moving through the fluid at velocity v, the impulses tend to oppose the motion (as discussed above) and we expect the average impulse μ_p will be proportional to v and opposite in sign. This tells us that the average collisional force $\mu_p/\Delta t$ is the x-component of the viscous drag force. Then from Eq. 4 we have

$$\frac{\mu_p}{\Delta t} = -\gamma v \tag{6}$$

How does a Brownian particle slow down or speed up due to μ_p and δp? How does this produce an average kinetic energy in agreement with the equipartition theorem? The particle's kinetic energy changes because the final momentum $p_f = p + \Delta p = p + \mu_p + \delta p$ differs from the initial momentum $p = mv$. The energy change is given by

$$\begin{aligned}\Delta E &= \frac{p_f^2}{2m} - \frac{p_i^2}{2m} \\ &= \frac{1}{2m}\left((p + \mu_p + \delta p)^2 - p^2\right) \\ &= \frac{1}{2m}\left(\mu_p^2 + \delta p^2 + 2p\delta p \right. \\ &\qquad \left. + 2\mu_p p + 2\mu_p \delta p\right)\end{aligned} \tag{7}$$

This energy change can be non-zero over any interval Δt; the particle can gain or lose energy in the short term. However, if the particle is to remain in thermal equilibrium over the long term, the average energy change should be zero. Applying the equilibrium condition $\langle \Delta E \rangle = 0$ will allow us to relate the variance of δp to factors associated with μ_p. Therefore we need to evaluate the expectation value of the right side of this expression, which is simply the sum of the expectation values of each term:

$$\begin{aligned}\langle \Delta E \rangle &= \frac{1}{2m}\Big(\langle \mu_p^2 \rangle + \langle \delta p^2 \rangle + 2\langle p\delta p \rangle \\ &\qquad + 2\langle \mu_p p \rangle + 2\langle \mu_p \delta p \rangle \Big)\end{aligned} \tag{8}$$

Note first of all that the third term on the right side is $2\langle p\delta p\rangle = 2m\langle v\delta p\rangle$. Because the particle velocity v and the random part of the collisional impulse δp are statistically independent, the expectation value of their product is the product of their expectation values: $\langle v\delta p\rangle = \langle v\rangle\langle \delta p\rangle$. This term is zero because δp is a zero-mean random variable. The same applies to the last term in the parentheses, which contains the product $2\langle \mu_p \delta p\rangle$. Because δp is random and uncorrelated with μ_p, this term will also be zero.

The first term on the right side involves μ_p^2, where we have already noted that μ_p is proportional to the time interval Δt. Therefore this is the only term in the expression that varies as Δt^2, while every other term is proportional to Δt. Since we can choose Δt as small as we like, we can make this term arbitrarily small in comparison to the other terms. We can safely discard this term as an insignificant contribution to $\langle \Delta E\rangle$.

Now we can use Eq. 6 relating the viscous drag behavior and μ_p. Making the substitution $\mu_p = -\gamma v \Delta t$, we have the expectation value of the fourth term in Eq. 8: $2\langle \mu_p p\rangle = -2\gamma\Delta t\langle vp\rangle = -2m\gamma\Delta t\langle v^2\rangle$. This term and the remaining $\langle \delta p^2\rangle$ term then give

$$\begin{aligned}\langle \Delta E\rangle &= -\gamma\langle v^2\rangle \Delta t + \frac{\langle \delta p^2\rangle}{2m} \\ &= -\gamma\frac{k_B T}{m}\Delta t + \frac{\langle \delta p^2\rangle}{2m}\end{aligned} \tag{9}$$

where in the last line we used the equipartition theorem applied to the particle's mean square velocity: $\langle v^2\rangle = k_B T/m$.

Setting $\langle \Delta E\rangle = 0$ and solving for $\langle \delta p^2\rangle$ then gives

$$\langle \delta p^2\rangle = 2\gamma k_B T\,\Delta t \tag{10}$$

Note this agrees with the prior assertion that $\langle \delta p^2 \rangle$ should be proportional to Δt. Moreover it gives the proportionality constant, $2\gamma k_B T$, that is needed to keep the average velocity in agreement with the equipartition theorem. Although derived for a particle moving along the x-axis, this same expression will apply to each of the three dimensions, and so we find the desired connection between the viscous drag coefficient, the mean squared random impulse (along any axis), and the temperature (i.e. the thermal equilibrium condition).

Equation 10 leads directly to a version of the *fluctuation-dissipation theorem*, which says that the variance of the fluctuating force must be proportional to the dissipative drag coefficient γ and $k_B T$. To see this, write the total collisional force as

$$\begin{aligned} F_c(t) &= \frac{\Delta p}{\Delta t} \\ &= \frac{\mu_p}{\Delta t} + \frac{\delta p}{\Delta t} \\ &= F_{\text{drag}}(t) + F(t) \end{aligned} \tag{11}$$

where $F(t) = \delta p / \Delta t$ and, since δp is a zero-mean Gaussian random variable with a variance given by Eq. 10, $F(t)$ will be a zero-mean Gaussian random variable with a variance

$$\left\langle F^2(t) \right\rangle = \frac{2\gamma k_B T}{\Delta t} \tag{12}$$

$F(t)$ is called the Brownian force. In equilibrium, and on average, the energy lost by the particle to the fluid via the drag force $F_{\text{drag}}(t)$ is balanced by the energy gained by the particle from the fluid via the fluctuating Brownian force $F(t)$.

Note that different values of δp over any non-overlapping time intervals arise from a different set of collisions and thus will be statistically independent. For example, even for adjacent time intervals, the two δp values would be equally likely plus as minus. This independence implies $F(t)$ is uncorrelated in time with $\langle F(t) F(t') \rangle = 0$, for $t \neq t'$ (or, at least, for $|t - t'| > \Delta t$). Thus, $F(t)$ is a very odd force that fluctuates virtually instantaneously on all but the shortest time scales.

The local environment may produce other forces on a small particle. The silica particles in our experiment can adhere to a glass coverslip. A vesicle in a plant cell may be pulled through the cell by a molecular motor, while a swimming bacterium generates its own propulsion force by spinning its flagella. These additional forces compete with the trapping and fluid forces. If these forces are known, measurements of the displacements they cause can be used to determine the strength of the trap. If the trap strength is known, measured displacements can be used to determine these additional forces. Subsequent sections describe how to use the physics of Brownian motion and viscous drag to determine the strength of the trapping and drag forces.

We will need to know the position x of the particle with respect to the trap. In principle we could calculate x by analyzing microscope images collected with a camera. In practice this does not work well because the displacements are very small and fluctuate rapidly. We can obtain higher precision and faster time resolution if we detect the particle's displacement indirectly by measuring the laser light that the particle deflects from the beam focus. Light scattered by the particle travels downstream (along the laser beam axis) and—in our apparatus—is measured on a quadrant photodiode detector (QPD). The QPD is discussed in the experimental section. Here we merely note that as the particle moves within the trap in either the $+x$ or $-x$-direction, it deflects some of the laser light in the same direction and the QPD reports this deflection by generating a positive or negative voltage V.

For small displacements x of the particle from the beam focus, the QPD voltage is linear

in the displacement ($V \propto x$). Consequently, we can write

$$x = \beta V \tag{13}$$

We will refer to β (units of meters/volt) as the *detector constant*. Because the voltage generated by the QPD depends on the total amount of scattered light, β depends on the laser power as well as the shape and size of the particle and other optical properties of the particle and liquid.

Analysis of Trapped Motion

How can we measure the strength of the trap? Suppose that a particle, suspended in water, is held in the optical trap. If we move the microscope stage (that holds the sample slide) in the x direction at a velocity $\dot{x}_{\text{drive}}$, the water (sealed in the slide) will move at that same velocity. The water moves with the slide and does not slosh around because it is confined in a thin channel and experiences strong viscous forces with the channel walls. On the other hand, the trap (whose position is determined by the beam optics) will remain fixed so that the fluid and the trapped particle will then be in relative motion. The drag force is opposite the relative velocity and thus given by $-\gamma(\dot{x} - \dot{x}_{\text{drive}})$. Like the Brownian force, the viscous force is well-characterized and together they will serve as calibration forces for the trap as described next.

Together with the viscous force above, the trapping force $-kx$, and the Brownian force $F(t)$, Newton's 2nd law then takes the form

$$m\ddot{x}(t) = F(t) - kx - \gamma(\dot{x} - \dot{x}_{\text{drive}}) \tag{14}$$

where m is the particle mass and x is its displacement with respect to the equilibrium position of the trap.

Macroscopically the drag coefficient γ is related to the viscosity of the fluid and the size and shape of the moving particle. For a sphere of radius a, γ is given by the Einstein-Stokes formula

$$\gamma = 6\pi\eta a \tag{15}$$

where η is the dynamic viscosity of the fluid. While this equation is accurate for a spherical particle in an idealized fluid flow environment, the damping force is influenced by proximity to surfaces (the microscope slide) and is sensitive to temperature and fluid composition through the viscosity η. Thus it is appropriate to determine γ experimentally and compare it with the Stokes Einstein prediction. A complete calibration includes a determination of the trap stiffness k, the detector constant β, and the drag coefficient γ.

We use the calibration method designed by Tolic-Norrelykke, et al. The basic idea is to drive the stage back and forth sinusoidally with a known amplitude and frequency and measure (via the QPD detector voltage V) the particle's response to the three forces. Because the physics of heavily damped motion of a particle in a fluid are well understood, the frequency characteristics of $V(t)$ will reveal the parameters k, β, γ with good precision.

You are probably familiar with underdamped oscillators, for which the drag term $-\gamma\dot{x}$ in Newton's law is small in comparison to the acceleration ("inertial") term $m\ddot{x}$. For such oscillators the acceleration is largely determined by the other (nonviscous) forces acting on the particle. However, the drag coefficient γ in a fluid generally scales as the radius a of the particle, whereas the mass m scales with the particle's volume, $m \propto a^3$. Consequently, for sufficiently small particles ($a \sim \mu$m), the inertial term is far smaller than the drag term, $|m\ddot{x}| \ll |\gamma\dot{x}|$. Under such conditions, the oscillator is strongly over-damped and (to an excellent approximation) we may drop the inertial term from Eq. 14. The particle velocity is then determined by the balance between the viscous force and the other forces

acting on the particle. Physically this means that, if any force is applied to the particle, the particle "instantly" (see *Exercise 3* below) accelerates to its terminal velocity in the direction of the applied force. When we drop the $m\ddot{x}$ term, the equation of motion becomes quite a bit easier to work with:

$$F(t) = kx + \gamma(\dot{x} - \dot{x}_{\text{drive}}) \tag{16}$$

Exercise 3 *Suppose that the drag force $-\gamma\dot{x}$ is the only force acting on the particle so that the equation of motion becomes $m\ddot{x} = -\gamma\dot{x}$. Solve this equation for $\dot{x}(t)$ for a particle with an initial velocity v_0. Show that the velocity decays exponentially to zero and give an expression for the time constant involved. (This would also be the time constant for reaching terminal velocity when there are additional forces acting on the particle.) What is the time constant for a 1 μm diameter silica sphere moving through water ($\eta \simeq 10^{-3}$ N-s/m^2)? Integrate your solution for $\dot{x}(t)$ (assuming $x_0 = 0$) to determine $x(t)$. If the sphere has an initial velocity $v_0 = 1$ cm/s, approximately how far does it travel before coming to rest? Give your answer in microns (μm).*

Dropping the $m\ddot{x}(t)$ term in Eq. 14 is equivalent to assuming that the time constant for reaching terminal velocity is negligible. To solve the resulting Eq. 16, first collect the x and $\dot{x}$ terms on the right side and multiply throughout by $e^{kt/\gamma}$

$$\begin{aligned}(F(t) + \gamma\dot{x}_{\text{drive}})\, e^{kt/\gamma} = \\ \gamma\left((k/\gamma)\, x e^{kt/\gamma} + \dot{x} e^{kt/\gamma}\right)\end{aligned} \tag{17}$$

Recognizing the right hand side as a derivative, we find

$$x(t) = x_T(t) + x_{\text{resp}}(t) \tag{18}$$

where

$$x_T(t) = \frac{1}{\gamma}\int_{-\infty}^{t} F(t')e^{2\pi f_c(t'-t)}\, dt' \tag{19}$$

$$x_{\text{resp}}(t) = \int_{-\infty}^{t} \dot{x}_{\text{drive}}\,(t')\, e^{2\pi f_c(t'-t)}\, dt' \tag{20}$$

and

$$f_c = \frac{k}{2\pi\gamma} \tag{21}$$

has units of frequency (oscillations per unit time).

Equations 18-21 show that the motion $x(t)$ has two components due to two sources. $x_T(t)$ is the response to the random Brownian force $F(t)$ and $x_{\text{resp}}(t)$ is the response to the motion of the surrounding fluid. They are integrals of the past values of the source terms with an exponentially decreasing weighting factor having a damping time, $1/2\pi f_c$, determined by the ratio of the damping constant to the spring constant. This time constant is typically in the millisecond range and thus only recent past values contribute.

Applying a constant velocity flow (via a flow cell) so that $\dot{x}_{\text{drive}} = v_0$ creates a constant drag force γv_0 and causes a shift in the particle position $x_{\text{resp}} = \gamma v_0/k$. This is one common way to get information about the trap parameters γ and k. Our apparatus uses an oscillatory flow $\dot{x}_{\text{drive}}$ and looks for the predictable oscillatory response in $x(t)$ to provide the same information.

Thus, the microscope stage (i.e., the fluid) will be driven back and forth sinusoidally with a known amplitude A and frequency f_d. The location of the stage x_{drive} (with respect to the trap) is then given by

$$x_{\text{drive}}(t) = A\cos(2\pi f_d t) \tag{22}$$

and the fluid has a velocity

$$\dot{x}_{\text{drive}}(t) = -A2\pi f_d \sin(2\pi f_d t). \tag{23}$$

Exercise 4 *Derive Eqs. 18-20 above. Evaluate the integral for $x_{resp}(t)$ given a constant velocity flow $\dot{x}_{drive} = v_0$ and show that it produces the expected shift: $x_{resp}(t) = \gamma v_0/k$. Also evaluate the integral given the drive velocity of Eq. 23 and show that $x_{resp}(t)$ will be a sinusoidal oscillation at the same frequency with an amplitude given by*

$$A' = \frac{A}{\sqrt{1 + f_c^2/f_d^2}} \tag{24}$$

Because $F(t)$ is random, $x_T(t)$ is random—non-periodic and noisy. To characterize such signals, a statistical approach is typically used in which the frequency components of $x(t)$ are analyzed. For that we need to return to Eq. 16 and investigate the Fourier transform of the motion.

Consider the Fourier transforms of a trajectory $x(t)$

$$\widetilde{x}(f) = \int_{-\infty}^{\infty} x(t)\, e^{-2\pi i f t}\, dt \tag{25}$$

and of the Brownian force $F(t)$

$$\widetilde{F}(f) = \int_{-\infty}^{\infty} F(t)\, e^{-2\pi i f t}\, dt \tag{26}$$

The Fourier transform is evaluated for frequencies f covering both halves of the real axis $-\infty < f < \infty$ so that the inverse Fourier transform properly returns the original function. For example, $x(t)$ is recovered from the inverse Fourier transform of $\widetilde{x}(f)$:

$$x(t) = \int_{-\infty}^{\infty} \widetilde{x}(f)\, e^{2\pi i f t}\, df \tag{27}$$

Note that $\widetilde{x}$ has units of m/Hz and $\widetilde{F}$ has units of N/Hz.

A relationship between $\widetilde{x}$ and $\widetilde{F}$ is readily obtained by taking the Fourier transform of the equation of motion, Eq. 16. That is, multiply both sides by $\exp(-2\pi i f t)$ and integrate over dt. The result is

$$\widetilde{F} = k\widetilde{x} + \gamma 2\pi i f \widetilde{x} + \frac{2\pi\gamma f_d A}{2i}\left(\delta(f + f_d) - \delta(f - f_d)\right) \tag{28}$$

To get Eq. 28, the Fourier transform of $\dot{x}(t)$ has been replaced by $2\pi i f$ times the Fourier transform of $x(t)$—as can be demonstrated by evaluating $\dot{x}(t)$ starting from Eq. 27. The explicit form of $\dot{x}_{\rm drive}$ as given by Eq. 23 has been used and the Fourier transform of $\sin(2\pi f_d t)$, which is given by $(\delta(f - f_d) - \delta(f + f_d))/2i$, has been applied. Solving for $\widetilde{x}$ then gives

$$\widetilde{x}(f) = \frac{\widetilde{F}}{2\pi\gamma\,(f_c + if)} - \frac{f_d A}{2i\,(f_c + if)}\left(\delta(f + f_d) - \delta(f - f_d)\right) \tag{29}$$

where we have replaced k by $2\pi\gamma f_c$ (Eq. 21).

Equation 29 is a perfectly good description of the particle response x—it just happens to be Fourier transformed. We will use it to extract information from measurements of $x(t)$.

Discrete Fourier transforms

Although we have treated time t as a continuous variable that spans the range $-\infty \to +\infty$, in actual experiments we collect a finite number of data values over a finite time interval τ. A typical data set is a discrete sampling of the QPD voltage $V(t) = \beta x(t)$ over a time interval $\tau \simeq 1 - 2$ sec, with measurements acquired at a uniform digitizing rate R around 100,000 samples per second, i.e., with a time spacing between data points $\Delta t = 1/R$. For this discussion, we can consider β as given, so that the data consists of values of $x(t_m)$ at a set of uniformly-spaced sampling times t_m.

Let's assume that measurements of $x(t)$ are made during the time interval from $-\tau/2 <$

$t < \tau/2$. The integration in Eq. 25 needs to be truncated so that t falls within this interval only. Of course, we expect to recover the predicted results in the limit as $\tau \to \infty$.

To analyze finite, discrete data sets, we need to define the *discrete Fourier transform* (DFT). The DFT of $x(t)$ is the version of the Fourier transform that is comparable to Eq. 25 but applies to a large (but finite) number L of discretely sampled $x(t_m)$ values. If the measurement times t_m are spaced $\Delta t = \tau/L$ apart in time and the integration is over the range $-\tau/2 \le t \le \tau/2$, then we can write $t_m = m\Delta t$ with $-L/2 \le m \le L/2$. The finite integration corresponding to Eq. 25 is performed according to the rectangle rule and becomes

$$\widetilde{x}(f_j) = \sum_{m=-L/2}^{L/2} x(t_m) e^{-2\pi i f_j m \Delta t} \Delta t \qquad (30)$$

The DFT is expected to accurately reproduce the true Fourier transform with some well understood limitations discussed shortly.

The DFT is evaluated at fixed frequencies $f_j = j\Delta f$ where

$$\Delta f = \frac{1}{\tau} \qquad (31)$$

and $-L/2 \le j \le L/2$. That is, both $x(t)$ and its DFT $\widetilde{x}(f_j)$ contain the same number of points, but each of the $\widetilde{x}(f_j)$ has both a real and an imaginary part. However, the two parts are not independent. If the $x(t)$ are real (as is the case here), it is easy to demonstrate (from Eq. 26) that $\widetilde{x}(-f) = \widetilde{x}^*(f)$. That is, for opposite frequencies, f and $-f$, the real parts are equal and the imaginary parts are negatives of one another. Thus $x(t_m)$ and $\widetilde{x}(f_j)$ both contain the same number of independent quantities. The two sets are just different ways of representing the same data.

The power spectrum

Another issue arises because the theory of Brownian motion does not specify $\widetilde{F}(f)$. At any frequency, $\widetilde{F}(f)$ is complex (since $e^{-2\pi i f t} = \cos 2\pi f t - i \sin 2\pi f t$). For any complex number $z = x + iy = re^{i\theta}$, x and y are the real and imaginary parts of z, r is the modulus and $\theta = \arctan(y/x)$ is the argument or phase of z. The theory only predicts the *intensity* given by the modulus squared: $r^2 = x^2 + y^2 = zz^*$, where $z^* = x - iy$ is the complex conjugate of z. It does not predict the real or imaginary parts of z individually or the phase. Moreover, the theory predicts that the Fourier intensities $\widetilde{F}\widetilde{F}^*$ obtained from a finite Fourier transform will be proportional to the integration interval τ. The theory thus gives a result that is independent of τ only if the intensities are divided by τ. The traditional characterization of the strength of a real, fluctuating function of time, such as the Brownian force $F(t)$ is its (two-sided) *power spectrum* or *power spectral density* (PSD), defined as

$$P_F(f) = \frac{\widetilde{F}(f)\widetilde{F}^*(f)}{\tau} \qquad (32)$$

defined for both positive and negative frequencies. As with $x(t)$, $F(t)$ is real and therefore $\widetilde{F}(-f) = \widetilde{F}^*(f)$. This implies that $P_f(-f) = P(f)$ and for this reason the power spectrum at f and $-f$ is often added together to create the one-sided power spectrum. The power spectrum at $f = 0$ is left unmodified. It arises from any nonzero (DC offset) in the corresponding quantity. For a Brownian force $P_F(0)$ is expected to be zero as there is no long term average force in any direction.

For $f \neq 0$, the power spectrum of the Brownian force is actually expected to be a constant—independent of f. That $P_F(f)$ is flat and extends out to high frequencies is a result of the collisional origin of the Brownian

force as described previously. Furthermore, in order that the average speed of the particle obeys the equipartition theorem (Eq. 2), the one-sided PSD must depend directly on both the temperature T and the viscous drag coefficient γ:

$$P_F(f) = 4\gamma k_B T \tag{33}$$

Equation 33 is another way of expressing the fluctuation-dissipation theorem of Eq. 10. Here, it gives the relationship between γ and the PSD for the fluctuating Brownian force.

For any frequency component f of a given trajectory $x(t)$, $\widetilde{x}(f)$ is also a complex random variable with a mean of zero. The square of its Fourier transform, $\widetilde{x}\,\widetilde{x}^*$, will have a non-zero mean and, as with $\widetilde{F}\,\widetilde{F}^*$, is also proportional to the integration time τ. Thus the power spectral density for $\widetilde{x}$ is

$$P(f) = \frac{\widetilde{x}(f)\widetilde{x}^*(f)}{\tau} \tag{34}$$

and is also independent of τ.

Again, because $\widetilde{x}(-f) = \widetilde{x}^*(f)$, $P(-f) = P(f)$ and, as with the power spectrum $P_F(f)$, we add the components at f and $-f$ (and leave the component at $f = 0$ as is) to create the one-sided power spectrum defined for positive f only. This one-sided power spectrum, which we still call $P(f)$, is then fit to the predictions for $f > 0$ given next. (We don't fit at $f = 0$, as this component arises from any DC component in $x(t)$ and is typically an artifact of imperfectly positioning of the QPD.)

To derive the predicted relationship between the one-sided power spectra for $x(t)$ and $F(t)$, consider the case where the stage oscillations are turned off; $A = 0$ and the delta functions in Eq. 29 are gone. With only the Brownian force contributing, multiply each side of Eq. 29 by its complex conjugate, divide by τ, and add negative and positive frequency components to get

$$\begin{aligned} P(f) &= \frac{P_F(f)}{4\pi^2\gamma^2(f_c^2 + f^2)} \\ &= \frac{k_B T}{\pi^2\gamma(f_c^2 + f^2)} \end{aligned} \tag{35}$$

where Eq. 33 was used to eliminate $P_F(f)$. (From here on, all power spectra are the one-sided variety.)

Notice that $P_F(f)$ has units of N^2/Hz and $P(f)$ has units of m^2/Hz. It makes sense to consider these functions as a squared amplitude per unit frequency. For example, if we integrate $P(f)$ over a sufficiently small interval Δf centered around a frequency f_0, we obtain $P(f_0)\Delta f$. Using the one-sided PSD means this value would represent the mean squared amplitude $A^2/2$ of the oscillatory component of $x(t)$ at the frequency f_0.

If the stage oscillations are turned back on, how do they affect the power spectrum? We can refer to Eq. 29 and see how the two delta function terms (resulting from the stage motion of amplitude A at the drive frequency f_d) contribute. The inverse Fourier transform of the delta function term in Eq. 29 shows that it represents oscillations at the drive frequency f_d with an amplitude A'

$$A' = \frac{A}{\sqrt{1 + f_c^2/f_d^2}} \tag{36}$$

(This result was derived in *Exercise 4* from the response integral of Eq. 20. Here we see it can be obtained using Fourier transforms as well.) The case $f_c \ll f_d$ corresponds to a weak trap or high drive frequency and gives $A' = A$; the amplitude of the particle oscillation equals the amplitude of the stage oscillation. For stronger traps or lower drive frequencies, Eq. 36 shows how the trap attenuates the oscillation of the particle relative to that of the stage; A' is smaller than A by the factor of $\sqrt{1 + f_c^2/f_d^2}$.

Therefore the power spectrum of the particle in the trap is the sum of two terms.

$$P(f) = \frac{k_B T}{\pi^2 \gamma \left(f_c^2 + f^2\right)} + \frac{A^2}{2\left(1 + f_c^2/f_d^2\right)} \delta\left(f - f_d\right) \quad (37)$$

$$= P_T(f) + P_{\text{resp}}(f) \quad (38)$$

where $P_T(f)$ is the first term—the power spectrum without stage oscillations (Eq. 35) and $P_{\text{resp}}(f)$ is the second term—the δ-function term. These two terms have the noteworthy behaviors discussed next.

P_{resp} is such that its integral over any frequency interval that includes f_d gives the mean squared amplitude $A'^2/2$ of the particle's sinusoidal response to the applied stage oscillations.

With the trap off ($k = 0$, $f_c = 0$) and so $P_T(f) = k_B T/\pi^2 \gamma f^2$, i.e., it falls off as $1/f^2$. With the trap on ($f_c \neq 0$), f_c plays the role of a "cutoff frequency." At high frequencies $f \gg f_c$, f_c can be neglected compared to f and once again, $P_T(f) = k_B T/\pi^2 \gamma f^2$—the same as for the trap off; high-frequency oscillations are unaffected by the trap. At low frequencies $f \ll f_c$, f can be neglected compared to f_c and $P_T(f) = k_B T/\pi^2 \gamma f_c^2$. The power spectrum goes flat (becomes independent of f) and does not continue increasing as f decreases. Moreover, this low-frequency amplitude decreases as $1/f_c^2$, i.e., the amplitude of the motion at low frequencies decreases as the trap strength increases. Finally, $P_T(f)$ increases with temperature and decreases with γ; fluctuations in the position of the particle are larger at higher temperatures and are suppressed by the viscous drag.

Equation 37 is for the particle's position x, while we will actually measure the QPD voltage $V(t) = x(t)/\beta$. Our experimentally determined power spectrum density will be that of the voltage $\widetilde{V}\widetilde{V}^*/\tau$, not the position $\widetilde{x}\widetilde{x}^*/\tau$. As the Fourier transform is linear, the Fourier transform of $V(t)$ is related to that of $x(t)$ by the calibration factor β:

$$\widetilde{V} = \widetilde{x}/\beta \quad (39)$$

Accordingly, if we experimentally measure $V(t)$ and then calculate $P_V(f)$, the PSD of the voltage data, then we expect

$$P_V(f) = P(f)/\beta^2 \quad (40)$$

Keep in mind that the main prediction, Eq. 37, for $P(f)$ was derived from continuous Fourier transforms assuming an infinite measurement time, whereas our data are collected in a discrete sampling over a finite interval τ. Because the discrete power spectrum $P_V(f_j)$ is derived from a finite set of $V(t_m)$ collected over a time interval τ spaced Δt apart, it is not expected to perfectly reproduce that prediction. However, the differences due to the finite acquisition time and sampling rate are well understood and predictable.

One aberration is aliasing. The highest frequency represented in $P_V(f_j)$ is at $j = L/2$ or $f_j = \Delta f L/2$, which is just half the sampling rate and called the *Nyquist frequency* f_{Ny}. If the true power spectrum is zero for all frequencies above f_{Ny}, then $P_V(f_j)$ should agree well with the true $P_V(f)$ at all f_j. However, if the true $P_V(f)$ has components above f_{Ny}, these components show up as artifacts in $P_V(f_j)$. Components in the true $P_V(f)$ at frequencies near $f' = f_{\text{Ny}} + \delta f$ show up in the discrete version $P_V(f_j)$ at frequencies f_j near $f_{\text{Ny}} - \delta f$; the true components are reflected about the Nyquist frequency. For example, for a 200 kHz sampling rate, the Nyquist frequency is 100 kHz and oscillations in $V(t)$ at 104 kHz, show up in $P_V(f_j)$ near $f_j = 96$ kHz. The effects of aliasing will be apparent in your data and can be dealt with easily.

The randomness of the trajectory over the finite time interval leads to power spectra that

have random variations from the predictions—the PSDs will be noisy. The noise would decrease as we work toward the limit $\tau \to \infty$. However, it is not practical to take ever longer measurements, with correspondingly larger data sets. Data sets larger than a few hundred thousand data points are tedious to manage and analyze; the improvement in the result does not justify the extra effort of handling and processing such large data arrays. A far better way to approach the limit of $\tau \to \infty$ experimentally is just to collect a number of data sets of duration $\tau \sim 1$ sec and then average the $P(f)$ obtained from each set.

After each τ-sized $V(t)$ is measured, its discrete Fourier transform $\widetilde{V}(f_j)$ is calculated and then used to determine its power spectrum density $P_V(f_j)$. After sufficient averaging of such $P_V(f_j)$, the predicted behavior will begin to appear—a continuous part from $P_T(f)$ and a sharp peak at f_d due to $P_{\rm resp}(f)$. This averaged PSD is fit to the prediction of Eq. 37 (with Eq. 40) to determine the parameters of the optical trap: the trap constant β, the drag coefficient γ and the force constant $k = 2\pi\gamma f_c$.

Exercise 5 *In the optical trapping literature, typical reported values for the cutoff frequency are in the range $f_c \simeq 10^2 - 10^3$ Hz. Assuming that these correspond to 1 μm diameter spherical particles in water at room temperature (295 K), estimate the magnitude of the trap stiffness constant k. For $f_c = 100$ Hz, what displacement would result if the full weight of a 1 μm diameter silica sphere hung from a spring with this force constant?*

The equipartition theorem also applies to the average potential energy of a harmonic oscillator:

$$\left\langle \frac{1}{2} k x^2 \right\rangle = \frac{1}{2} k_B T \qquad (41)$$

Use this relation to find the rms deviation of the particle from its equilibrium position: $\sqrt{\langle x^2 \rangle}$. Compare this rms displacement and the size of the shift in the equilibrium position due to gravity/buoyancy, with the particle diameter.

Exercise 6 *Make two sketches of the $P_T(f)$ term in Eq. 37 for a particle in a trap with f_c = 100 Hz. The first sketch should use linear scales (P_T vs. f), while the second should use a log-log scale ($\log P_T$ vs. $\log f$) for $10^{-2} f_c \leq f \leq 10^2 f_c$.*

Comparing the predicted $P_V(f)$ with one actually determined from the measured QPD voltage vs. time data is done in two steps: one for the thermal component $P_T(f)$ and one for the delta function response $P_{\rm resp}(f)$. We will begin with a discussion of the latter.

The main theoretical feature of a delta function is that its integral over any region containing the delta function is one. Thus, the predicted integral W of the $P_V(f)$ of Eq. 40 associated with the delta function in Eq. 37 is easily seen to be

$$\begin{aligned} W &= \frac{1}{\beta^2} \int_0^\infty P_{\rm resp}(f)\, df \\ &= \frac{A^2}{2\beta^2 \left(1 + (f_c/f_d)^2\right)} \end{aligned} \qquad (42)$$

In the experiment, the drive frequency f_d will be chosen so that there will be an exact integer number of complete drive oscillations over the measurement interval τ. This makes f_d one of the frequencies at which the $P_V(f_j)$ is evaluated and should produce one high point in this PSD. You will determine the height of that point above the thermal background and multiply by the spacing Δf between points to get the experimental equivalent of integrating $P_V(f)$ over the delta function. In rare cases, you may see the experimental delta function spread over several f_j centered around f_d. In these cases, the experimental integral is the

sum of the amount these points exceed the thermal background times Δf.

The experimental value of W obtained this way is then used with Eq. 42 and the known stage oscillation amplitude A, the drive frequency f_d, and the value of f_c (determined in the next step) to determine the trap constant β.

The force constant k and the drag coefficient γ are found by fitting the non-δ-function portion of the experimental $P_V(f)$ ($f \neq f_d$) to the prediction of Eq. 37 (with Eq. 40). That is, for all values of f except $f = f_d$, the predicted PSD can be written

$$P_V(f) = \frac{k_B T}{\pi^2 \beta^2 \gamma \left(f_c^2 + f^2\right)} \tag{43}$$

For fitting purposes, this equation is more appropriately expressed

$$P_V(f) = \frac{B}{1 + f^2/f_c^2} \tag{44}$$

where B is predicted to be

$$B = \frac{k_B T}{\pi^2 \beta^2 \gamma f_c^2} \tag{45}$$

The experimental $P_V(f_j)$ is then fit to Eq. 44 over a range of f (not including the point at $f = f_d$) which then determines the fitting parameters B and f_c.

With f_c determined directly from this fit, the experimental W is used with Eq. 42 to determine β. Then, if we assume T is equal to the measured room temperature, the fitted B can be used in Eq. 45 with f_c and β to determine the value of γ. Finally, the force constant $k = 2\pi\gamma f_c$ (Eq. 21) is determined and the three trap parameters γ, β and k are then known.

Apparatus

Overview

Our optical trap is based on the design of Appleyard et al. The design uses an inverted microscope to focus an infrared diode laser beam onto the sample and detects the deflection of that beam with a quadrant photodiode detector (QPD). The design also illuminates the sample with white light and generates an image of the sample on a video camera. The details are somewhat complex, as the same optical elements perform several functions simultaneously. The layout is described below. Refer to Fig. 2 while considering the following two optical paths:

The optical path for the infrared laser: The diode laser is a semiconductor device that outputs its ($\lambda = 975$ nm) infrared beam to a single-mode optical fiber. A converging lens (#1) receives the diverging light exiting the fiber and collimates it to a beam with a diameter of ~ 10 mm, or sufficient to fill the back aperture of the trapping objective (#3). A pair of mirrors and the dichroic mirror (#2, infrared-reflecting) are used to steer the laser beam vertically upward, along the central axis of the objectives. The beam enters the back aperture of the lower microscope objective (#3) (100× Nikon 1.25 NA, oil-immersion), which brings the beam to a focus at the sample, forming the optical trap. The upper microscope objective (#4) captures and re-collimates the infrared light that has passed through the sample and directs this energy upward. A dichroic (infrared-reflecting) mirror (#5) then deflects the beam toward a converging lens (#6), which focuses the beam onto the quadrant photodiode detector (#7, QPD).

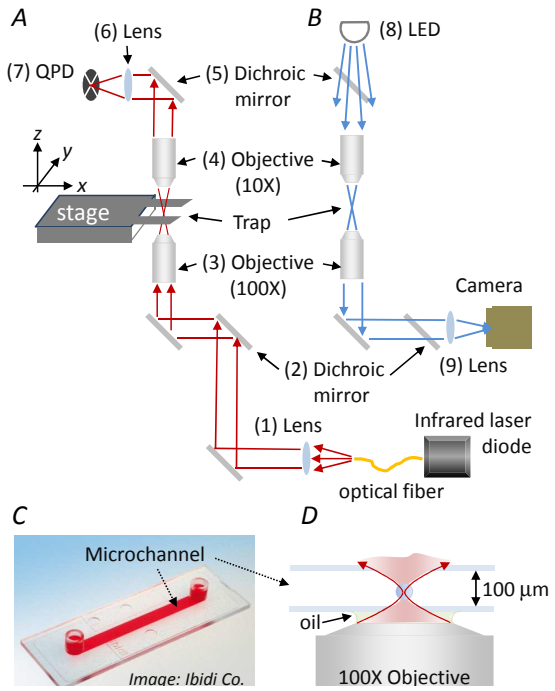

Figure 2: *A* and *B* show two views of the optical system, illustrating the paths of the infrared trapping rays (red arrows in *A*) and the visible illumination rays (blue arrows in *B*) as they pass through the same optical elements. The sample is contained in a 100 µm-deep microchannel slide *C*, at the focus *D* of the 100× oil-immersion lens.

The optical path for visible light: An LED (#8) generates white light that passes through the dichroic mirror (#6) and is focused by the upper objective (#4) onto the sample. Transmitted light from the sample area near the trap is gathered by the lower objective (#3) and with lens (#9) is brought to an image at the camera.

In this design the infrared laser serves two roles. It traps the particle at the focus, and it is also used to detect the motion of the particle within the trap. If there is no particle in the trap, the infrared laser beam propagates along the optical axis of the instrument, i.e., along the common cylindrical axis of the microscope objectives). The recollimated beam exiting the upper objective travels parallel to the optical axis, and converging lens #6 brings this beam to a focus just a bit in front of the center of the QPD. However, if a small particle is near the laser focus, the beam is refracted away from the optical axis. The collimated beam leaving the upper objective will then propagate at an angle to the optical axis, and so it is focused by converging lens #6 to a spot that is displaced from the center of the QPD. The QPD reports this displacement as a voltage V, which is proportional to the particle's displacement x from the laser focus (see Eq. 39). The QPD actually detects deflections in the both the x and y directions, reporting two independent voltages V_x and V_y that you will measure.

Hardware

Data acquisition board

The computer communicates with the tweezers apparatus via a USB connection or through a (National Instruments PCI-MIO-16E-4) multifunction data acquisition board (DAQ) located inside the computer. See Figure 3.

The DAQ board supplies voltages that move the positioning stage in the xy plane and it reads voltages from the quadrant photodiode—the raw data for analyzing particle motion in the trap. Two components of the DAQ board are used to do these tasks—an analog to digital converter (ADC) and two digital to analog converters (DACs).

The ADC and both DACs are 12-bit versions, meaning they have a resolution of 1 part in $2^{12} = 4096$ of their full scale range. For example, on a ±10 V range setting, voltages are read or written to the nearest 4.88 mV. An amplifier in the DAQ allows for full scale ranges on the ADC from ±10 V to ±50 mV.

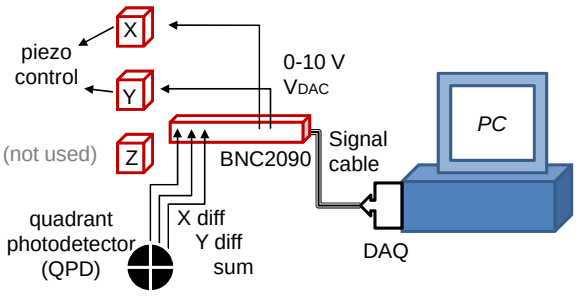

Figure 3: Schematic of electronic interface between computer and tweezer apparatus. The DAQ board in the PC has an analog-to-digital converter that reads data from the QPD, as well as digital-to-analog converters that supply control voltages for the xy positioning of the microscope stage.

The DAC range is ± 10 V. The ADC can read analog voltages at speeds up to 500,000 readings per second, and the DACs can write output voltages at similar speeds. The ADC has a high speed switch called a multiplexer that allows it to read voltages on up to eight different inputs.

A cable connects the DAQ card in the PC to an interface box (National Instruments BNC-2090) that has convenient BNC jacks for connecting coaxial cables between the various apparatus components and the DAQ input and output voltages.

Laser

The laser diode package (Thorlabs, PL980P330J) is premounted to a single-mode fiber which brings the laser light to the apparatus. The package is mounted on a temperature stabilized mount (Thorlabs, LM14S2) kept at constant temperature by the (Thorlabs, TED200C) temperature controller. An interlock requires the temperature controller to be on before the laser current controller will operate. The laser current is adjusted and stabilized by a current controller (Thorlabs, LDC210C). The laser current can be read off the controller. The laser turns on at a threshold current around 70 mA and then the laser power increases approximately linearly with current over threshold.

Internal to the laser diode package, a small, constant fraction of the laser beam is made to fall on a photodiode which generates a current proportional to the laser beam power. This current is measured in the laser current controller and can be read if you set the front panel meter to display I_{PD}. The supply allows you to scale I_{PD} with any proportionality constant for display as P_{LD}. By independently measuring the actual laser power P out of the 100× objective as the laser current is varied, the proportionality between P and I_{PD} was confirmed and the proportionality constant has been adjusted so that P_{LD} gives the laser power P out of the objective. Of course, P will not be P_{LD} if the beam path is blocked or if the alignment of the laser is changed. The instructor should be involved if a new calibration is deemed necessary.

Controller hub

There are six Thorlabs "T-Cube" electronic modules mounted in the (Thorlabs, TCH-002) T-Cube controller hub. The modules, described below, are used to electronically control the position of the microscope slide and to control and read the quadrant photodiode detector. The hub supplies a signal path between different modules and between all six modules and the computer's USB bus.

Quadrant Photodiode Detector

A quadrant photodiode detector (Thorlabs, PDQ80A) is used to produce voltages that are linearly related to the position of a particle in the neighborhood of the laser focus. It has

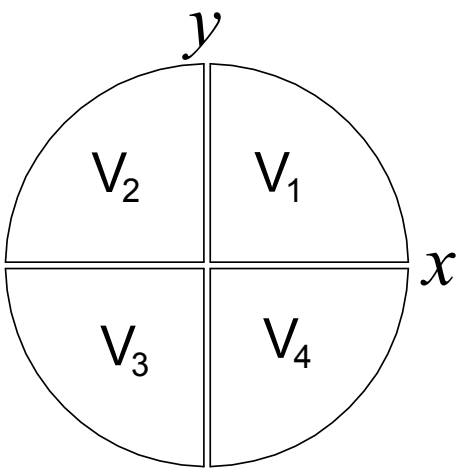

Figure 4: The QPD measures the intensity on four separate quadrant photodiodes.

four photodiode plates arranged as in Fig. 4 around the origin of the xy-plane. The plates are separated from one another by a fraction of a millimeter and extend out about 4 mm from the origin. The QPD receives the infrared light from the laser and outputs a current from each quadrant proportional to the power on that quadrant.

The Thorlabs TQD-001 module powers the QPD and processes the currents. It does not output the currents directly. Instead, it converts them to proportional voltages V_1-V_4 by additional electronics to produce the following three output voltages. The x-diff voltage is the difference voltage $V_x = V_1 + V_4 - (V_2 + V_3)$, the y-diff voltage is $V_y = V_1 + V_2 - (V_3 + V_4)$ and the sum voltage is the sum of all four. V_x is thus proportional to the excess power on the two quadrants where x is positive compared to the two quadrants where x is negative. Similarly for the y-diff voltage. The sum voltage is proportional to the total laser power on all four photodiodes.

With no scattering, the light that is brought to a focus by the 100× objective diverges from there and is refocused by the 10× objective and lens #6 so that it again comes to a focus just a bit in front of the QPD. The rays diverge from this focus before impinging on the photodiodes so that by the time they get there, the spot is a millimeter or two in diameter and when properly centered will hit all four quadrants equally.

With a particle in the trap, the scattered and unscattered light interfere and produce an interference pattern on the QPD that depends on the location of the scatterer. For small variations of the particle's position from equilibrium, the QPD voltages V_x and V_y produced by these patterns are proportional to the particle's x and y positions. That is $x = \beta V_x$ and $y = \beta V_y$.

While the range of linearity between the V and x is quite small—on the order of a few microns, it is still large compared to the typical motions of a particle in the trap (see *Exercise 5*). Significantly, this voltage responds very quickly to the particle's position so that high frequency motion (to 100 kHz or more) is accurately represented by $V(t)$.

The QPD module has buttons for control of its function and it has an array of LEDs that show whether the beam intensity pattern is striking the QPD roughly in the center (center LED lit) or off-center (off-center LEDs lit). The QPD is mounted on a manually-controlled, relatively coarse xy stage that will be centered by hand during calibration.

Microscope stage and piezoelectric control

The microscope stage is the component that supports the microscope slide between the 100× and 10× objectives. It is built around the Thorlabs MAX311D 3-axis flexure stage, which provides three means for positioning the slide in the trapping beam.

First, and very crudely, you can manually slide the stage across the table, for coarse positioning in the x- and y-directions. You will need to do this to put your slide into the beam, but you will find it difficult to position the sample to better than about ± 1 mm using this method.

Second, the stage has a set of micrometers that can be turned manually to move the stage. Over a range of about 300 μm, the micrometers operate as differential screws, in which two internal threads with slightly different pitches turn simultaneously—producing a very fine translating motion around 50 μm/revolution. As you continue turning the micrometer spindle, the differential operation runs out and the motion switches to a coarser control in which the stage moves around 500 μm/revolution. The coarse control can be obtained directly by turning the micrometers at the knurled ring up from the spindle, which then bypasses the differential screw.

Third, inside the stage there are three piezoelectric stacks that allow the computer to move the stage along each of the x, y and z axes. Piezoelectrics ("piezos") are crystals that expand or contract when voltages are applied across two electrodes, which are deposited on opposite sides of the crystal. The Thorlabs TPZ-001 piezo controller modules supply these control voltages (up to about 75 V). The piezos provide very fine and precise control of stage motion, but only over short distance ranges: The full 75 V range generates only about 20 μm of stage motion. The piezo voltage can be read from an LED indicator on the face of the module, which also has control buttons and a knob for the various modes of controlling this voltage.

There are several ways to use the piezo controller. Manual mode, in which the voltage is controlled via the knob on the module, will be disabled and is not used in our setup. (The differential micrometers are far more convenient manual controls.) Only the following two electronically controlled methods will be used.

One method is to use the DACs to supply analog voltages in the range of 0-10 V to the Thorlabs piezo-control module. The Thorlabs module amplifies these voltages to the 0-75 V scale and sends them to the piezo. This is the fastest method and is the main one used in our apparatus. Alternatively, the computer can communicate with the control module over the USB bus to request a desired piezo voltage.

Unfortunately, piezos have strong hysteresis effects. Their length, i.e., how far they will move the stage, depends not only on the present electrode voltage, but also on the recent history of this voltage. One method to deal with piezo hysteresis is to obtain feedback data from a strain gauge mounted alongside the piezo. The stage has one strain gauge for each of the three axes. They are read by the Thorlabs TSG-001 strain gauge modules, which are placed next to the matching piezo module in the controller hub.

The strain gauge is a position transducer with an output voltage that is very linear in the displacement caused by the corresponding piezo. The output voltage from the strain gauge module is internally wired to its corresponding piezo module through the controller hub. The displacement of the strain gauge caused by the piezo is indicated on a scale on top of the strain gauge module in units of percentage of the full scale: 0-100% for motion of about 20 μm.

Using strain gauge feedback, the controller allows you to supply USB commands requesting stage positions as a percentage (0-100) of the full scale motion (i.e., 0-100% of 20 μm). This is the second mode of motion control used in this experiment. Electronic feedback circuitry adjusts the actual voltage sent to the

piezo to achieve that percentage on the strain gauge. Our setup has only two strain gauge controllers, which are used only on the x and y piezos. (We do not use the z-piezo.)

Another issue with the stage is cross talk between the x, y and z motions of the stage due to its flexure design. The stage is capable of roughly 4 mm of travel in each direction, but the motions can couple to one another. Right around the middle position of the stage, changing x, y or z piezo or micrometer, should only move the stage in the x, y or z direction. However, as you move away from this central position, changing the x-piezo or micrometer, for example, will not only change the x-position of the stage; the flexure design causes small changes in the y and z-positions as well. In addition, the motion calibration factors—how much stage motion will correspond to a given micrometer or piezo change will change. For example, when the stage is near the limit in one or more of the three directions (± 2 mm), changing the x piezo, say, will move the stage in the y- and z-directions by as much as 30% of the amount moved in the x-direction. Consequently, it is worthwhile to try to operate the stage near the middle of its x, y and z ranges.

Camera

A Thorlabs DCU-224C color video camera is used to observe and monitor the happenings in the trap. It is also the means for transferring a length scale from a calibration slide to the motion caused by the piezo. The camera has a rectangular CCD sensor with pixels arranged in a 1280×1024 cartesian grid with 5.3 μm spacing. Thus distances measured on the image in pixels will scale the same way in x and y with real distances on the slide.

Software

UC480

The camera is controlled and read using the UC480 software program. This program has features for drawing or making measurements on the images, and for storing frames or video sequences. Select the Optimal Colors option at load time, then hit the Open camera button—the upper left item on the upper toolbar. The default camera settings generally work fine, but if there are image problems, many camera settings can be adjusted to improve image quality.

Note that there is a bad light path in our apparatus that throws some non-image light onto the camera sensor. This artifact can be eliminated by partially closing the adjustable aperture directly under the camera.

Become familiar with the measurement tools and the drawing tools on the utility toolbar arrayed along the left edge of the screen. In particular, you will use the Draw circle, Draw line, and Measure tools. Other settings and features can be found on the upper toolbar or the menu system. Start with the contrast and white balance set for automatic optimization. Learn how to set and clear an AOI or *area of interest* (a rectangular area on the sensor) so that only the data from that area is sent from the camera to the program. This increases the frame rate compared to using the full sensor.

Initialize program

This program sets up all the T-Cube modules to run in the appropriate modes used in other programs. It sets the piezo and strain gauge feedback channel, zeros the piezos' outputs and then zeros the strain gauges. Finally, it sets the x- and y-piezos near their midpoint voltages of 37.5 V, and sets the oper-

ating mode to add this 37.5 V to the voltages generated by signals applied to the external input. In this way, the piezo is near the middle of its extension, and so both positive and negative translation in x and y can be generated by supplying positive or negative DAC voltages to the back of the piezo controller.

Oscillate Piezo program

This program creates sinusoidal waveforms from the two DACs for driving the x-and y-inputs of the piezo controllers. It is used in conjunction with the UC480 Camera program to calibrate the amplitude of the stage motion when driven by a waveform of a given amplitude and frequency.

Raster Scan program

This program is used to scan the x- and y-piezos in a slow scan mode using strain gauge feedback while time averaging the signals from the QPD. The raster scan starts with a fixed voltage applied to the x-piezo while the y-piezo is scanned back and forth over a user-defined range. Then the x-piezo is moved a small amount in one direction and the y-piezo is scanned again. This move-x-and-scan-y process is repeated until the x-piezo has also scanned over the user defined range. At each xy value, the program digitizes the V_x and V_y signals from the QPD module and displays the results for each of these signals.

This program is used to see how the QPD works, give a sense for the intensity pattern on the QPD, determine an approximate detector constant β, and see how β depends on both the laser intensity and objective focusing.

Tweezers program

The main measurements are made from this program. It has two tabbed pages along the right. One is labeled Acquire and is for setting the data acquisition parameters, measuring the V_x and V_y signals from the QPD, and computing and averaging the PSD. The other tab is labeled Fit and is for fitting the PSD to the predictions of Eq. 37.

The default parameters for data acquisition should work fine. The number of points in each scan of V_x and V_y vs. t is forced to be a power of 2 ($2^{18} = 262144$ is the default) so that fast Fourier transforms can be used. The sampling rate (number of readings per second) for the ADC is determined by dividing down a 20 MHz clock on the DAQ board. The divisor is the number of 20 MHz clock pulses between each digitization. The maximum speed of the ADC is around 250 kHz when reading two channels (V_x and V_y). The 105 default value for this divisor leads to a sampling rate around 190 kHz. With 2^{18} samples in each scan, each scan lasts $2^{18} \cdot 105/(20 \times 10^6\,\text{Hz}) = 1.38$ s. The inverse of this time (0.73 Hz) is the frequency spacing between points in the PSD.

The ADC has an instrument amplifier that allows bipolar full scale (F.S.) voltages from ± 50 mV up to ± 10 V. The F.S. range control should be set as small as possible without letting the V_x or V_y signals hit the range limits.

The two DACs used to drive the stage piezos send discretized sinusoidal waveforms with adjustable amplitudes and with an adjustable phase between them. You can set the amplitude A_x or A_y to zero to get one-dimensional back and forth stage motion. However, it is recommended that the amplitudes be set equal with a 90° phase difference so that the stage will move with nearly circular motion. This way no matter what direction the QPD's x and y responses are aligned to, the stage motion will be sinusoidal with the chosen amplitude in those directions.

Recall that the drive frequency for the stage must be made equal to one of the discrete

points in the QPD power spectrum. For this to happen there must be exact integer number M of stage oscillations spanning the data acquisition time. The default settings for this number is 32 and, with a data acquisition time of 1.38 s, gives a drive frequency $f_d = 23.2$ Hz (point 32 of the PSD).

The output waveform is constructed with 512 ($= 2^9$) points per period of the sinusoid. This is the maximum on-board buffer size for each DAC and is not adjustable. The program must then calculate a separate (integer) divisor of the 20 MHz clock that determines the output rate for each point on this output waveform. In order for M periods of the output waveform to be exactly equal to the total sampling time for the ADC, M must have common factors with the clock divisor for the ADC. For example, if the default divisor (for the ADC) of $3 \cdot 5 \cdot 7 = 105$ is used, allowed values for M would be any that can be made with single factors of 3, 5, and 7 and any number of factors of two. As a second example, an ADC divisor of $5 \cdot 5 \cdot 4 = 100$ gives a sampling rate of 200 kHz and allowed values of M will be any that can be made with one or two factors of 5 and any number of factors of two. Selecting disallowed values for M (those that would produce a non-integer clock divisor) will disable the continue button.

Once the data acquisition parameters have been accepted—by hitting an enabled continue button—they cannot be changed without restarting the program. One exception is the amplitude and phase of the drive waveforms. They can be adjusted by setting the new values in the controls for them and hitting the change amplitude button.

The fitting routine, accessed from the fit tab, has several features designed for the data from this apparatus. First note the channel selector just above the graph. It is used to switch between the two channels (0 or 1, i.e., the QPD x- or y-directions). The two cursors on the graph must be set to determine the points in between that will be used in the fit to Eq. 44. The PSD is normally displayed on a log-log scale, but this can be changed using the tools in the scale legend at the lower left of the graph. Our PSDs show that many high frequency and some low frequency noise components are being picked up in the V_x and V_y signals. They might originate from external light sources, electrical interference, table and apparatus vibrations, etc. These unwanted signals typically appear as spikes on top of the normal Lorentzian shape of the PSD.

Spikes at the high frequency end of the PSD can be eliminated from consideration by setting the second cursor below them. In fact, fits that include too many high frequency data points tend to take too long. Be sure to include enough points above f_c, but set the high cursor so there are less than 50,000 points in the fit. Spikes between the cursors can be eliminated from the fit by setting their weighting factors to zero. This is done programmatically by telling the program how to distinguish these spikes from the normal Lorentzian data. The criteria for eliminating the spikes thus requires an understanding of the normal and expected noise in the PSD.

Ordinary random variations in $V(t)$ over any finite time interval lead to noise in the Lorentzian PSD that becomes smaller as more data is averaged. Watch $P_V(f)$ as you average 50 scans and then stop the acquisition. Note that the size of the noise (not the unwanted spikes) on the vertical log scale is nearly constant. While the band of noise may appear a bit wider at higher frequencies, this is at least partially an artifact of the log f scale for the horizontal axis; at higher frequencies the points are more closely spaced so that the number of 2-sigma and 3-sigma variations appear more frequently per unit length along the

f-axis.

Uniformly sized noise on a log scale implies the fractional uncertainty in $P_V(f)$ is constant. Estimate the ±1-sigma fractional uncertainty that would include about 68% of the data points in any small region of frequency. As you probably noticed above, this fraction becomes smaller as more data is averaged. Check that it is roughly constant for all f even as $P_V(f)$ varies by one or more orders of magnitude. Enter this fraction in the control for frac. unc. (fractional uncertainty). Then enter the rejection criterion in the reject control. For example, setting the frac. unc. control to 0.1 indicates that near any f, 68% of the $P_V(f)$ data points should be within ±10 percent of the middle value. Setting the reject control to 3 would then exclude from the fit (set the weights to zero) any points more than 30% "off."

The program uses the fitted PSD at any f as the central value for the rejection. For example, with the settings given above, any points more than 30% from the current estimate of the fitted curve would be thrown out. The initial guess parameters define the current estimate of the fitted $P_V(f)$ according to Eq. 44, and these estimates must be set close enough that good points are not tossed. Click on the show guess button to see the current estimate of the fitted $P_V(f)$ and the resulting rejected points, which are shown with overlying ×'s. Clicking on the do fit button initiates a round of nonlinear regression iterations excluding the rejected points. After the fitting routine returns, click on the copy button to transfer the ending parameter values from the fit to the initial guess parameters and display the new points that would be rejected in another round of fitting. Continue clicking the copy and then the do fit buttons until there are no further changes in the fit.

$P_V(f)$ varies over several orders of magnitude and the fact that the fractional uncertainty is roughly constant over a wide range, indicates even the points out in the tails of the Lorentzian contain statistically significant information. If an equally weighted fit were used, the points in the tails would not contribute to the fitting parameters as their contribution to the chi-square would be too small compared to the points at lower frequencies where $P_V(f)$ is much larger. Consequently, the fit should not be equally weighted. Because the data point y-uncertainties σ_i are proportional to y_i, the fit uses weights $1/\sigma_i^2$ proportional to $1/y_i^2$. If the fitting function accurately describes the data and the correct fractional uncertainty is provided, the normalized deviations between the data and the fit $(y_i - y_i^{\text{fit}})/\sigma_y$ should be approximately Gaussian-distributed with a mean of zero and a variance of one and the reduced chi-square for the fit should be about one.

Check the graph of normalized deviations to verify the expected behaviors and check for systematic deviations. (Click on the alternate tab control for the graphs to find this graph.) This graph also shows excluded points and can also be used to make sure valid points are not being rejected. Even though the rejection criteria depends only on the product of the frac. unc. and reject controls, the frac. unc. control should be adjusted to get a reduced chi-square around one and the reject control should be adjusted so that only undesired points are rejected from the fit. Correctly setting both controls really only matters if you are interested in determining the fitting parameter uncertainties. Recall that the fitting parameter covariance matrix scales with the assumed covariance matrix for the input y_i. With σ_i set proportional to y_i, setting the fractional uncertainty to get a reduced chi-square of one determines the proportionality factor to use in order to get the best estimates for the true

input and output covariance matrices.

Experimental overview

The basic tasks are to measure the trap strength, calibration constant, and drag coefficient for small particles of silica (SiO_2) roughly 0.5-1.5 μm in diameter. Having gained this experience with the apparatus, you can then experiment with biological trapping by measuring, e.g., the force generated by a swimming bacterium.

Note that it takes a couple of days to prepare the bacterial culture for this experiment, so you will need to plan ahead by notifying your instructor of the date when you plan to perform the bacterial study.

Laser Safety

Note that although this experiment is not dangerous, any eye exposure to the infrared laser beam would be very dangerous. The beam is very intense, with a power of several hundred mW, and it is invisible. Serious and permanent eye injury could result if the beam enters your eye. **Proper laser eye safety precautions must be used at any time that the laser is running.**

The apparatus is designed to keep the infrared laser beam enclosed within its intended optical path and away from your eyes. The instrument is safe to use as long as the laser remains enclosed. Therefore, laser safety means that you should not operate the laser when the beam enclosure is open or any portion of the optical pathway has been opened or disassembled. If you open or disassemble any components while the laser is powered you could expose yourself to the IR beam and suffer a potentially severe injury. Do not attempt to align or adjust any part of the infrared laser optical path.

The only point in the apparatus where the beam leaves its confining path is at the sample slide, between the two microscope objectives. In this region the beam is strongly converging/diverging and is not likely to present a hazard to the user. However you should use common sense and avoid diverting the beam out of this region. Do not place shiny, metallic or reflective objects like mirrors or foil into that region. Do not put your face close to the slide if the laser is on.

General concerns

In addition to laser safety issues, please take care to observe the following precautions

- *Alignment of the optical system:* All optical elements have already been carefully aligned and optimized. The only optical adjustments you will need to make involve the xyz positioning of the microscope stage and xy positioning of the QPD. **Do not attempt to move, disassemble or adjust the optical fiber or any of the mirrors and lenses and other optical components.** If you disturb the laser alignment, the optical trap will cease to function and it will require tedious and time-consuming realignment. Any disassembly of the apparatus could also lead to accidental and very dangerous eye exposure to the laser beam.

- *The 100× objective:* Please take care that nothing (except immersion oil and lens paper) ever touches the lens of the lower microscope objective. In focusing or adjusting the stage you should not crash or scrape the slide against the lens.

- *The laser optical fiber:* Please do not touch or handle the optical fiber. It is extremely delicate and costly to repair.

- *The laser settings:* The laser beam power is adjustable up to a maximum current of $I_{LD} = 650$ mA. The laser also has a temperature controller that has been programmed to maintain the laser at its optimum temperature. You can adjust the laser current right up to the maximum limit value, but please do not attempt to change the limit or the laser control temperature.

Procedures

The following procedures should probably be done in the order outlined below. They will take more than one day. Be sure to follow the procedures in the *Cleaning Up* section before leaving.

Initialization

Turn on the power supply for the controller hub. Wait a few seconds for their firmware to initialize and then run the Initialize program. Check that the LED light source is on.

Camera calibration

Find the Thorlabs R1L3S3P grid slide and determine which side has the grid patterns. Place a small drop of immersion oil over the smallest (10 μm) grid pattern and place the slide on the sample stage with the calibration markings facing downward (oil side down). Then *carefully* slide the stage into position over the objective, watching that you do not crash the slide into it: the bottom of the slide should be above the objective.

Start the UC480 camera program. Using the manual z micrometer, lower the slide down while watching the camera image for the grid to come into focus. You will need to get the slide quite close to the objective lens (less than a mm) to get into focus.

[Putting a drop of oil on the coverslip, putting the slide onto the stage (coverslip down) and into the area just above the 100× objective will henceforth be referred to as "installing" the slide. "Uninstalling" will mean raising the stage, sliding it away from the trap, and removing the slide.]

The 10 μm grid is rather small and so coarse and fine adjustments in the x- and y-directions may also be needed just to get it into view. If you are having trouble finding it, be sure the slide is correctly oriented with the grid side down. You may want to find the focus with one of the larger grid patterns first.

Now you can determine the pixel calibration constant: How many microns at the sample area correspond to one pixel on the camera image? Note this is not the actual pixel size (5.3 μm/pixel), but rather that size divided by the magnification, or roughly 0.05 μm/pixel. Use the camera software measuring tool to determine the separation in pixels of known lengths on the grid slide. (The grid squares are 10×10 μm.) Our camera pixels are square and you should find the same values in the x- and y-directions. Determine the camera calibration constant in μm/pixel.

Next use the x- and y-micrometers on the stage to determine their sensitivity on the fine (differential) operation. The micrometer fine-control spindles are marked with 50 divisions per rotation. Because the distance moved for each division is somewhat variable, we will call them m-units; 50 m-units per rotation. Use the camera and grid markings to determine these fine-control m-units per actual distance moved. This calibration constant should be near 1 m-unit per μm of real motion. However, remember that this calibration can change a bit depending on how far the stage is from its central position.

Uninstall the grid slide, clean it with alcohol, wiping it gently with sheet of lens paper,

and place it back in its protective case.

Sample sphere preparation

You will need to prepare two solutions of 1.2 μm diameter silica beads. Since you will need to make measurements on a single sphere, getting their concentration correct is very important. Too few spheres and it will be difficult to find any. Too many and the spheres will interfere with one another during the measurements.

Have the instructor show you proper use of the pipettors and vortex mixer. Be sure to use the vortex mixer just before sampling from the stock solution, any intermediate solutions, and just before loading your final solution into the slide. The spheres tend to settle and the vortex mixer is needed to get them uniformly distributed in the suspending liquid. If you do not mix, the density of spheres will be wrong. Moreover, if you don't mix the main stock solution before taking a sample, you would be changing the concentration of the remaining stock solution.

Prepare approximately 1.5 ml of a 150:1 dilution of the stock solution of the 1.2 μm spheres in deionized (DI) water. Even this diluted solution is still much too dense for measurement and another 150:1 dilution is needed. For stuck spheres, this second dilution should be into 1M NaCl water, which makes them stick to the slide. For free spheres, use DI water again. Only make the free sphere dilution at this point. You may want to adjust the concentration for the stuck spheres. Be sure to mark the vials with the sphere size, dilution factor, date, and whether it is in water or a salt solution. At a dilution of $150^2 = 22,500$, there should be an average of a few beads in the camera image. If it turns out there are more than 10 beads per image area, further reduce the concentration.

The Ibidi slide has wells on each side where the solution is introduced. The first sample needed will be the 1:22,500 dilution in DI water. Put about 100 μl in one well and use a syringe to suck it through the channel, taking care not to suck air into the channel. (Add another 50 μl as the well empties.) It is easier to see the liquid coming into the channel if the slide is placed on a dark background. When filled, add or remove the solution to the wells as necessary to get it about half-way high in each well. If the heights are unequal, there will be a pressure difference which will drive the fluid from one well to the other until the pressure difference is eliminated. Even if you get the well heights equal by eye, small differences can still drive the fluid and it can take several minutes for the motion to cease. It can be very difficult to see spheres if they are moving with any but the smallest velocity flow.

Initial observation of a trapped sphere

Make sure the laser is off. Install the slide prepared above. As you bring the slide down, look for individual spheres undergoing Brownian motion. Spheres and small dirt particles will often become stuck to the coverslip at the bottom of the channel or to the glass at the top of the channel. Find these surfaces and measure their separation in m-units to be sure they are, in fact, the top and bottom of the 100 μm channel. Being certain the focus is in the channel and just above the top of the coverslip is often helpful in the hunt for free spheres. Spheres will be more dense at the bottom of the channel, but should be found higher up as well.

When you see spheres, turn on the laser to a current of approximately 400 mA and move the stage around manually as you try to capture a sphere into the trap. You will know that a particle is trapped because it will remain in

the same location and same focus, even as you adjust the stage from side to side as well as up and down. Mark the trap position on the video image with the circle tool on the camera software and save this drawing.

A particle trapped in the z-direction will not change its focus (appearance on the image) when you adjust the stage up and down in the z-direction. While you are moving the slide, the trapped particle's position is fixed because the laser focus is fixed relative to the $100\times$ objective. If you raise the slide enough, however, sooner or later the sphere will hit the bottom of the channel and then go out of focus if you continue raising the slide. Similarly, if you lower the slide enough, the sphere will hit the top of the channel. If the trap is weak, you may have problems keeping a sphere trapped near the top of the channel. Because of the optical properties of the objective and sample, the trap force in the z-direction is expected to weaken as the sphere height increases.

Play around with this configuration a bit. Is the sphere density about right? Can you keep a single sphere trapped for many minutes or do other spheres often wander in? While you can compare measurements from different spheres with nearly the same diameter, small variations in their trap constants will affect the comparisons. Their dependence on laser power, for example, is smoother when all measurements are from the exact same sphere. To avoid spheres from wandering into an already filled trap, reduce the sample concentration. Setting it so there is about one sphere per camera image typically is about right. Working a bit higher in the channel helps in this regard as well.

Check the top and bottom z-micrometer positions as you demonstrate a trapped sphere can be moved from top to bottom of the channel. Save a short video sequence of an isolated, trapped sphere. Be sure you have recorded the trap position with a circle and have saved it as a drawing. It will be needed in later procedure steps.

Always be sure to make measurements at least 20 μm from the bottom of the channel. Viscosity effects cause the motion of the liquid around the spheres to change when the spheres are close to the bottom or top surface of the channel. Beyond 20 μm or so, the surfaces are effectively infinitely far away as far as viscosity effects go.

Uninstall the slide, empty it and refill it with an appropriate dilution of spheres in salt water to get, at most, a few per screen. This "stuck sphere" slide will be used in the next procedure.

Piezo calibration

You will next determine motion calibrations involving the use of the piezo controls on the stage. To do a piezo calibration requires observing a small object, such as a sphere, stuck to the slide. Install the slide prepared above and find a relatively isolated single sphere stuck to the coverslip.

The direct DAC method of driving the piezo is used in the main Tweezers program where the stage is set into sinusoidal oscillations of known frequency and amplitude. Consequently, a calibration constant—from the amplitude of the DAC drive voltage to the amplitude of the stage motion is needed. To perform this calibration, use the Oscillate Piezo program, which allows for convenient adjustments of the two DAC sinusoidal voltages. Their amplitudes as well as their common frequency and their phase difference are adjustable.

Because of the nonlinear piezo behavior, an applied sinusoidal voltage of amplitude V_{DAC} will cause nearly sinusoidal oscillations of the position with an amplitude A that depends nonlinearly on V_{DAC}. Run the Oscillate Piezo

program while viewing a stuck sphere. With the V_{DAC} at zero, the piezo doesn't move and the amplitude of the stage motion is zero. As you increase V_{DAC}, the stage motion amplitude increases in a near-linear fashion with a small quadratic component.

$$A = a_1 V_{\mathrm{DAC}} + a_2 V_{\mathrm{DAC}}^2 \tag{46}$$

If you apply equal amplitude oscillations to both the x- and y-piezos and set them 90° out of phase with one another, the stage should move in a circle with a radius given by Eq. 46. Or, you can set either the x- or y-oscillation amplitude to zero so that the stage moves back and forth in only one dimension. Use either method. Measure the amplitude A versus V_{DAC} in the range from 1 to 3.5 V at a 1 Hz frequency and fit that data to Eq. 46 to determine a_1 and a_2. Be sure that there is no constant term in the fit (as in Eq. 46) because the amplitude of the motion must be zero with no drive voltage. The peak-to-peak amplitude ($2A$) can be measured (in pixels) from camera images where you try to see and measure either the diameter of the circular motion or the extrema of linear oscillations. Be sure to measure to the center of the spheres—a task more difficult than it sounds as the extrema are often faint and blurred. These measurements are then converted to real stage motion by the pixel to stage distance factor determined from the previous grid pattern measurements. Setting a small AOI (area of interest) around the sphere will speed up the frame rate, which can be quite useful in this step.

Next, measure the stage amplitude with $V_{\mathrm{DAC}} = 1$ V at several drive frequencies up to 40 Hz. Then try it at 3-V drive amplitude. At higher frequencies, the stage accelerations for a given amplitude are larger and the stage inertia can affect the motion.

When measuring the PSD for particles in the trap, the stage oscillations will be in the 10-30 Hz range, but will be at very low amplitudes—a few tenths of a micron driven by a V_{DAC} of a few tenths of a volt. These oscillations are a bit too small to measure accurately with the camera. Instead, the calibration performed in this step should be extrapolated to these low amplitudes.

Leave the stuck-sphere slide mounted as it will be used in the next procedure.

QPD calibration

For the in situ calibration described in the theory section, the detector constant β will be determined from the PSD of a trapped sphere on an oscillating stage. It is nonetheless worthwhile to look at another method, described here, for determining β using a stuck sphere. This method shows why an in situ calibration is so much better and demonstrates some of the limitations involved in either calibration method.

Load the trap position drawing into the UC480 image and install the stuck-sphere slide. Move the slide so that there is a relatively isolated single sphere in the vicinity of the trap circle. Run the raster program. It starts in the calibration tab. Set the x and y strain gauge percentages in various combinations from 10 to 90% and measure the particle position on the camera for each x, y percentage requested. Check for proportional behavior between the motion and the percentage and determine the actual distance moved per strain gauge percent.

Turn on the temperature controller and then the laser current controller to about 400 mA. Move the slide in x and y so there are no beads within 10 μm of the trap circle, adjust the QPD xy-stage position to roughly zero the V_x and V_y signals from the QPD controller. Start with the ADC full scale range of ±10 V, but adjust it to the smallest range, once you

know how big V_x and V_y get. (Don't worry about keeping the sum voltage from saturating.) In the calibration tab, leave the sample ADC rate at 10,000 readings per second and averaging 500 such readings per point. This gives a 0.05 s averaging time or three cycles of the 60 Hz power lines. Using a multiple of 1/60 second reduces noise at 60 Hz.

Try the default scan parameters first: scan centered at 50% for x and y, scan range ±15% in x and y. The V_x and V_y data at each point in the scan are averaged according to the acquisition parameters above.

Manually move a relatively isolated, stuck sphere to the center of the trap circle. Adjust the z-focus so the sphere on the image appears about the way it did for a trapped sphere. Hit the Start Scan button. The camera should show how the raster scan proceeds and the program should go to the Acquire tab showing graphs of V_x and V_y vs. t as well as versus each other, which update with each scan line measured.

When the scan is complete, the program goes to the Analyze tab where you can see a 2-D "intensity plot" of V_y versus x and y on the left half and and V_x versus x and y on the right half. For an intensity plot, the values of V_x and V_y determine the plot color at each x, y value. Run the cursors through the center of the data in these plots to create the plots of V_x vs. x and V_y vs. y. These slices typically show oscillations as the sphere is scanned through the laser focal spot. You are trying to find the middle of the pattern where V_x vs. x and V_y vs. y demonstrate nearly straight-line behavior. Find the slopes in this region in V/x-unit and V/y-unit. Also check the range of the linear behavior in x- and y-units.

The x- and y-values on these graphs always range from 0-1. (Because of the way the graphs are stacked, x will range from 0-1 for the left intensity plot of V_y and from 1-2 for the right intensity plot of V_x. The range of 0-1 (or 1-2) will correspond to the full scale motion requested—30% for the default ±15% range. Divide your measured slope by the full scale range to get the slopes in V/% and then divide by strain gauge calibration factor in μm/% to get the slope in V/μm—the inverse of the QPD detector calibration constant β. Similarly convert the range for linear behavior to a true distance and compare with the expected rms displacements of a trapped particle as from *Exercise 5*.

Because the QPD voltages should all be proportional to the power on the detector and the power on the detector should be proportional to the overall laser power, the slopes in V/μm, say, should be proportional to the laser power. Check this by performing and analyzing a raster scan at half the laser power used above.

Measured this way (with a stuck sphere), β is very sensitive to how the sphere is positioned in the z-direction. When a floating sphere is trapped by the laser, it will oscillate somewhat in the z-direction because of the Brownian force, but its equilibrium position is at the center of the trap ($z = 0$) and cannot be adjusted. On the other hand, a stuck sphere can be placed anywhere in z by changing the z-position of the stage and its position will affect how well it will be focused on the camera. While your initial raster scan was at roughly the same focus as a trapped sphere, do another with the sphere moved slightly higher and/or lower (by changing the z-focusing) such that there is a modest change in the appearance of the image. Note how much the stage was moved, run another raster scan and and check how this affects β. What does this say about the assumption that β is a constant? How would a z-dependence to β affect the analysis?

Full trap calibration

Adjusting the piezos with the strain gauge feedback cannot always be done fast enough—particularly when applying an oscillatory motion to the stage as for the in situ calibration method. In this case, the computer's two DACs will be used to apply sinusoidal voltages directly to the input of the x and y piezo modules. The piezo module amplifies those voltages by about 7.5, adds them to the 37.5 V offset and sends them on to the actual piezotransducers in the stage.

Reuse or make a new slide with 1.2 μm spheres in DI water at an appropriate dilution to get about 1 sphere per CCD image. Install it between the objectives, find a trapped sphere and adjust the stage's z-position to get it about 30 μm above the coverslip.

Start the Tweezers program. Zero the x and y $V_{\rm DAC}$ amplitudes so the stage does not oscillate. Set the acquisition and timing parameters. Begin acquiring the QPD signal and averaging the calculated PSD $P_V(f_j)$. When it is sufficiently smooth, stop the averaging, switch over to the Fit tab and do a fit of the PSD to Eq. 44.

Turn on the piezo oscillation of the stage and set the $V_{\rm DAC}$ that would give a stage oscillation amplitude $A = 0.1 - 0.2$ μm. Begin averaging the PSD and perform a full analysis to determine β, γ and k. Repeat at different laser powers. Plot the trap strength k, the inverse of the calibration constant $1/\beta$, and the drag coefficient γ as a function of laser power. Discuss the results. Are k and $1/\beta$ directly proportional to laser power? Is γ constant? Can you see any systematic behavior with power? Why might this be reasonable?

Possible additional studies

Repeat the calibration procedure for other sphere sizes. Our largest are 5.1 μm in diameter and present several difficulties associated with their large size; they are about 75 times heavier than 1.2 μm spheres. We have spheres of diameter 0.5, 0.75, 1.0, 1.21, 1.5 and 5.1 μm. Most have not been studied. Except for the 1 μm spheres, the stock solutions are all 10% spheres by weight. Thus to get the same concentrations in particles per unit volume, the dilutions must scale in proportion to the the sphere volume—twice the sphere diameter, 1/8 as much dilution. Scaling laws for the parameters can be investigated.

Check out the Berkeley wiki for more information on the following two investigations, which are only briefly described here.

Investigate flagella locomotion in *E. coli* bacteria. You will have to prepare a dilution from a culture made one or two days before. Don't forget to request it well in advance. Normal *E. coli* repeatedly swim a bit and then tumble changing their direction from the tumble. We use a strain that has been genetically modified not to tumble—traveling more or less continually in one direction.

Make and install a slide with an appropriate dilution. This might take a few tries as it is difficult to predict the culture concentration. Capture a dead bacterium and use the Tweezers program to determine the trapping force. Then trap a swimming bacterium. Lower the laser power until it swims free. Repeat for other *E. coli* on your slide. What does the distribution (frequency histogram) of minimum laser powers look like? Does the length of time inside the trap affect the bacteria swimming strength? How well can you determine the swimming force generated by the bacterium from this measurement?

With the laser off, watch a swimming bacterium and determine their typical speeds. Estimate the size of the bacteria. Its *hydrodynamic radius* is that value of a that gives the actual drag force $F_d = -\gamma v$ when the Einstein-

Stokes formula (Eq. 15) is used with that a. Compare the two force determinations. Use your measurements to estimate the power generated by the flagellar motor of the swimming bacterium.

Investigate vesicle transport in onion cells. You will have to bring in your own onion. Be sure it is fresh—hard and tight, not mushy. Be sure to take any leftover onion home. Do not dispose it in the lab trash. It stinks up the room rather quickly.

Prepare a slide of onion epidermal cells in 0.1 M salt solution. Look for vesicles (bags of nutrients, waste or other cell material) floating in the cytoplasm and others traveling along specialized filaments. Find one and trap it. Move the slide to see if it is freely floating or stuck to a filament. How much can a filament stretch? What happens when you turn off the trap?

Trap one on a filament and watch as other vesicles back up along that filament. Turn off the trap and describe your observations. Trap an isolated vesicle on a filament and lower the laser power until it breaks free. Repeat for others vesicles on filaments. Is the minimum laser power the same every time? What might affect the distribution of minimum laser power. Are there other quantitative measurements you can make?

Cleaning Up

When finished for the day, shut off the laser temperature and current controllers. Close all open LabVIEW programs and then turn off power to the T-Cube hub. Most importantly, this turns off all voltages to the piezos. Leaving a voltage on the piezos over long periods can change their properties. Turn off the power strip so the LED will turn off as well. (The computer and monitors are on a separate power strip.)

Uninstall the slide, clean it with a Kim-Wipe and alcohol and use a syringe to run alcohol through the channel two or three times. Then fill it with alcohol and leave it in a 200 ml cylinder also filled with alcohol. This storage technique will keep the slide from becoming filled with bacteria or other living organisms and will help prevent breakage of the fragile coverslip. (If it is left full, as the water evaporates, the coverslip will often crack.) The Ibidi slides can be reused, but check the coverslip and dispose of the slide if it has more than a few small cracks.

Use a single sheet of **lens paper** (not a Kim-Wipe, which is very abrasive) to wipe the oil from the 100× objective. **Do not scrub.** Wipe gently once in one direction.

Clean up the apparatus and sample preparation area. Dispose of tissues in the trash can and dispose of glass or plastic slide material or pipettor tips in the disposal box by the sink.